

Southern Illinois University Edwardsville

SPARK

SIUE Faculty Research, Scholarship, and Creative Activity

Spring 3-29-2017

Synthesis, Structural Characterization and Catalytic Activity of Indenyl Complexes of Ruthenium Bearing Fluorinated Phosphine Ligands

Matthew J. Stark

University of Missouri-Saint Louis

Michael J. Shaw

Southern Illinois University at Edwardsville

Arghavan Fadamin

Southern Illinois University Edwardsville

Nigam P. Rath

University of Missouri-Saint Louis

Eike B. Bauer

University of Missouri-Saint Louis

Follow this and additional works at: https://spark.siu.edu/siue_fac

 Part of the [Inorganic Chemistry Commons](#)

Recommended Citation

Stark, Matthew J.; Shaw, Michael J.; Fadamin, Arghavan; Rath, Nigam P.; and Bauer, Eike B., "Synthesis, Structural Characterization and Catalytic Activity of Indenyl Complexes of Ruthenium Bearing Fluorinated Phosphine Ligands" (2017). *SIUE Faculty Research, Scholarship, and Creative Activity*. 119.
https://spark.siu.edu/siue_fac/119

This Article is brought to you for free and open access by SPARK. It has been accepted for inclusion in SIUE Faculty Research, Scholarship, and Creative Activity by an authorized administrator of SPARK. For more information, please contact magrase@siue.edu.

Synthesis, Structural Characterization and Catalytic Activity of Indenyl Complexes of Ruthenium Bearing Fluorinated Phosphine Ligands

Matthew J. Stark,^a Michael J. Shaw,^b Arghavan Fadamin,^b Nigam P. Rath,^{a,c} and Eike B. Bauer^{a,*}

Dedicated to Professor John A. Gladysz on the occasion of his 65th birthday.

^a *University of Missouri - St. Louis, Department of Chemistry and Biochemistry, One University Boulevard, St. Louis, MO 63121, USA.*

^b *Southern Illinois University Edwardsville, Department of Chemistry, Edwardsville, IL 62025, USA.*

^c *Center for Nanoscience, University of Missouri - St. Louis, One University Boulevard, St. Louis, MO 63121, USA.*

bauere@umsl.edu

To be submitted to the Journal of Organometallic Chemistry

Keywords: electronic tuning, X-ray, cyclic voltammetry, propargylic alcohols

Abstract

The synthesis, characterization and catalytic activity of new ruthenium complexes of fluorinated triarylphosphines is described. The new ruthenium complexes $[\text{RuCl}(\text{ind})(\text{PPh}_3)\{\text{P}(p\text{-C}_6\text{H}_4\text{CF}_3)_3\}]$ and $[\text{RuCl}(\text{ind})(\text{PPh}_3)\{\text{P}(3,5\text{-C}_6\text{H}_3(\text{CF}_3)_2)_3\}]$ were synthesized in 57% and 24% isolated yield, respectively, by thermal ligand exchange of $[\text{RuCl}(\text{ind})(\text{PPh}_3)_2]$, where ind = indenyl ligand $\eta^5\text{-C}_9\text{H}_7^-$. The electronic and steric properties of the new complexes were studied through analysis of the X-ray structures and through cyclic voltammetry. The new complexes $[\text{RuCl}(\text{ind})(\text{PPh}_3)\{\text{P}(p\text{-C}_6\text{H}_4\text{CF}_3)_3\}]$ and $[\text{RuCl}(\text{ind})(\text{PPh}_3)\{\text{P}(3,5\text{-C}_6\text{H}_3(\text{CF}_3)_2)_3\}]$ and the known complex $[\text{RuCl}(\text{ind})(\text{PPh}_3)_2]$ differed only slightly in their steric properties, as seen from comparison of bond lengths and angles associated with the ruthenium center. As determined by cyclic voltammetry, the redox potentials of $[\text{RuCl}(\text{ind})(\text{PPh}_3)\{\text{P}(p\text{-C}_6\text{H}_4\text{CF}_3)_3\}]$ and $[\text{RuCl}(\text{ind})(\text{PPh}_3)\{\text{P}(3,5\text{-C}_6\text{H}_3(\text{CF}_3)_2)_3\}]$ are +0.173 and +0.370 V vs. $\text{Cp}_2\text{Fe}^{0/+}$, respectively, which are substantially higher than that of $[\text{RuCl}(\text{ind})(\text{PPh}_3)_2]$ (-0.023 V). After activation through chloride abstraction, the new complexes are catalytically active in the etherification of propargylic alcohols (8 to 24 h at 90 °C in toluene, 1-2 mol% catalyst loading, 29-61 % isolated yields). As demonstrated by a comparative study for a test reaction, the three precursor complexes $[\text{RuCl}(\text{ind})(\text{PPh}_3)\{\text{P}(p\text{-C}_6\text{H}_4\text{CF}_3)_3\}]$, $[\text{RuCl}(\text{ind})(\text{PPh}_3)\{\text{P}(3,5\text{-C}_6\text{H}_3(\text{CF}_3)_2)_3\}]$ and $[\text{RuCl}(\text{ind})(\text{PPh}_3)_2]$ differed only slightly in catalytic activity.

1. Introduction

Transition metal complexes of ruthenium are widely utilized in catalysis and other areas of chemical research [1]. A large number of ruthenium complexes have been described in the literature, and they have found applications as catalysts in reactions such as oxidations [2], olefin metathesis [3], and a number of carbon-carbon, carbon-nitrogen and carbon-oxygen bond forming reactions [4]. The quest for sterically and electronically tuned ruthenium complexes is ongoing to satisfy the growing need of such complexes in the area of medicinal chemistry [5] and the development of optical devices [6].

The known [7] ruthenium indenyl complex $[\text{RuCl}(\text{ind})(\text{PPh}_3)_2]$ ($\text{ind} = \eta^5\text{-C}_9\text{H}_7^-$) has previously been utilized as a starting material for organometallic syntheses [8] and other ruthenium indenyl complexes are frequently applied in synthesis [9] and catalysis [10]. The increased reactivity of indenyl complexes has been ascribed to the so called “indenyl effect” [11]. As part of our long standing research program directed towards the catalytic activation of propargylic alcohols [12], we identified ruthenium indenyl complexes as valuable starting materials not only for the synthesis of ruthenium complexes [12a,c,f], but also as potential catalysts in nucleophilic substitution reactions [12a,c]. However, a serious drawback of these catalyst systems are the high reaction temperatures of 80 to 90 °C required for transformations. The high reaction temperatures are undesirable because of the energy required and the difficulties of obtaining high enantiomeric excess values under such conditions in addition to rearrangements that often occur as side reactions, lowering the yield of the desired product. We hypothesized that electron-withdrawing groups on the ruthenium center might increase its reactivity, as these groups might facilitate the nucleophilic attack on (potential) carbocation intermediates. Our previous electronic tuning efforts utilizing electron-withdrawing ligands resulted in the synthesis of the tris(*N*-pyrrolyl)phosphine complex $[\text{RuCl}(\text{ind})(\text{PPh}_3)\{\text{P}(\text{pyr})_3\}]$

(pyr = *N*-pyrrolyl, see Figure 1), which catalytically activated propargylic alcohols, albeit still at reaction temperatures around 85 °C [12a].

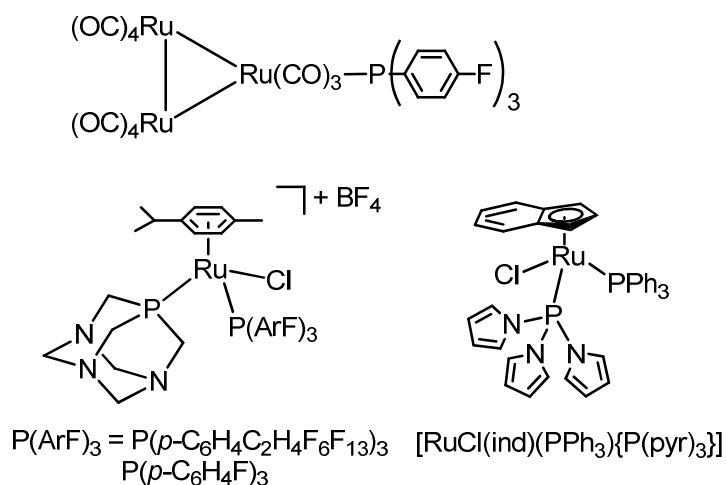


Figure 1. Representative electronically tuned ruthenium complexes.

Fluorinated phosphine ligands have previously been utilized to electronically tune ruthenium complexes, representative examples are shown in Figure 1 [13]. Ruthenium complexes bearing fluorinated phosphine ligands have been applied in catalysis [14] and also exhibited anticancer activity [15]. Fluorinated phosphines have also been employed in the synthesis of metal complexes to be employed for fluorous biphasic catalysis [16]; for example, Gladysz published fluorous analogs of Grubbs' second-generation catalyst to be employed in ring-opening metathesis polymerization [17]. In context of our own research, we hypothesized that ruthenium indenyl complexes bearing electron-withdrawing, fluorinated phosphine ligands show, due to their increased Lewis acidity, enhanced catalytic activity in the transformation of propargylic alcohols.

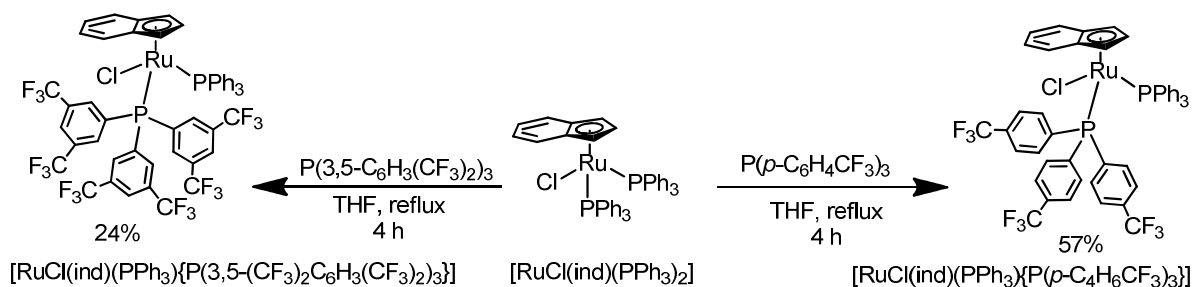
Herein, we describe the synthesis and characterization of the ruthenium complexes $[\text{RuCl(ind)(PPh}_3\text{)}\{\text{P}(p\text{-C}_6\text{H}_4\text{CF}_3)_3\}]$ and $[\text{RuCl(ind)(PPh}_3\text{)}\{\text{P}(3,5\text{-C}_6\text{H}_3(\text{CF}_3)_2)_3\}]$ where $\text{P}(p\text{-C}_6\text{H}_4\text{CF}_3)_3$ is tris(4-(trifluoromethyl)phenyl)phosphine and $\text{P}(3,5\text{-C}_6\text{H}_3(\text{CF}_3)_2)_3$ is tris(3,5-

bis(trifluoromethyl)phenyl)phosphine. We investigated the steric and electronic properties of the new complexes through X-ray analysis and cyclic voltammetry. The new complexes were demonstrated to be catalyst precursors for the etherification of propargylic alcohols. The catalytic activity of $[\text{RuCl}(\text{ind})(\text{PPh}_3)\{\text{P}(p\text{-C}_6\text{H}_4\text{CF}_3)_3\}]$, $[\text{RuCl}(\text{ind})(\text{PPh}_3)\{\text{P}(3,5\text{-C}_6\text{H}_3(\text{CF}_3)_2)_3\}]$ and $[\text{RuCl}(\text{ind})(\text{PPh}_3)_2]$ were compared and potential catalytically active species in the reaction mixture were investigated.

2. Results and Discussion

2.1. Ruthenium complex syntheses.

The known [7] ruthenium indenyl complex $[\text{RuCl}(\text{ind})(\text{PPh}_3)_2]$ has previously been utilized as a starting material for organometallic syntheses by us [12,18] and others [8], as one of the PPh_3 ligand can be thermally exchanged by other ligands. Accordingly, when the complex $[\text{RuCl}(\text{ind})(\text{PPh}_3)_2]$ was refluxed with one equivalent of either $\text{P}(p\text{-C}_6\text{H}_4\text{CF}_3)_3$ or $\text{P}(3,5\text{-C}_6\text{H}_3(\text{CF}_3)_2)_3$ in THF for four hours, the new complexes $[\text{RuCl}(\text{ind})(\text{PPh}_3)\{\text{P}(p\text{-C}_6\text{H}_4\text{CF}_3)_3\}]$ and $[\text{RuCl}(\text{ind})(\text{PPh}_3)\{\text{P}(3,5\text{-C}_6\text{H}_3(\text{CF}_3)_2)_3\}]$ were isolated chromatographically in 57 and 24% yields, respectively (Scheme 1). The low yields may be due to decomposition reactions that occur during reaction and workup, as little to no starting material was observed by NMR in the crude products.



Scheme 1. Synthesis of ruthenium complexes bearing fluorinated aryl phosphine ligands.

The new complexes were characterized by multinuclear NMR, MS, IR, elemental analysis and X-ray diffraction. In both complexes, the coordination of one fluorinated phosphine ligand and one PPh₃ ligand is readily indicated by two distinct ³¹P{¹H} NMR signals at 50.1 and 44.2 ppm and at 50.1 and 47.8 ppm, respectively. As expected for complexes with two magnetically different phosphorus atoms in the metal coordination sphere, coupling between the two signals was observed. Coupling constants ²J_{PP} of 42 Hz were determined.

In general, the indenyl ligand gives very distinct ¹H and ¹³C{¹H} NMR signals for the three protons and the five carbon atoms of its coordinated five-membered ring [19]. All these carbon and proton atoms of the indenyl ligand in the new complexes gave individual signals in the corresponding ¹H and ¹³C{¹H} NMR spectra.

2.2. X-ray structures

In order to unequivocally establish the structure of the new ruthenium complexes, the X-ray structures of [RuCl(ind)(PPh₃){P(*p*-C₆H₄CF₃)₃}] and [RuCl(ind)(PPh₃){P(3,5-C₆H₃(CF₃)₂)₃}] were determined (Figure 2). Selected bond lengths and angles are listed in Table 1, and for comparison purposes, the X-ray data for [RuCl(ind)(PPh₃)₂] [20] and for [RuCl(Ind)(PPh₃){P(pyr)₃}] (Figure 1) [12a] from the literature are also included. As previously observed by us [12a], it appears that complexes of the general formula [RuCl(ind)(PPh₃)L] are structurally not significantly different from the “parent” complex [RuCl(ind)(PPh₃)₂]. For the complex [RuCl(ind)(PPh₃){P(3,5-C₆H₃(CF₃)₂)₃}], a face-to-face aromatic donor-acceptor interaction between one of the fluorinated aryl rings and one of the phenyl rings of PPh₃ was

observed (Figure 2, bottom) [21]. The distance between the two aryl ring systems was calculated to be 3.873 Å.

The P-Ru-P and P-Ru-Cl bond angles around the ruthenium center range from 91.612(17)° to 99.585(19)°, and are also similar to the bond angles of the other two complexes listed in Table 1. The geometry of the new complexes is, thus, best described as slightly distorted octahedral. The somewhat increased P-Ru-P bond angles for the two new complexes indicates some steric repulsion of the PPh₃ and the fluorinated ligands. It appears that the bulkier phosphine P(3,5-C₆H₃(CF₃)₂)₃ forms a smaller P-Ru-P angle with PPh₃ compared to the less bulky phosphine P(p-C₆H₄CF₃)₃ which might be a consequence of the face-to-face interaction in the solid state shown in Figure 2. For the other two, structurally related complexes in Table 1, increased P-Ru-P bond angles between the phosphine ligands were observed as well.

The Ru-P bond lengths for the two new complexes range from 2.2696(5) to 2.3203(5) Å and are not appreciably different from each other. It appears that the electron-withdrawing character of the fluorinated ligands does not have a profound impact on the Ru-P bond lengths compared to the structurally related complexes [RuCl(ind)(PPh₃)₂] and [RuCl(Ind)(PPh₃){P(pyr)₃}] (Figure 1). Also, the distances between the centroids of the C5 ring of the indenyl ligands and the ruthenium centers for both complexes are similar (1.904 and 1.903 Å) and comparable to that for [RuCl(ind)(PPh₃)₂] (1.918 Å).

As can be seen from the X-ray structures, the indenyl ligands for both complexes are η⁵-coordinated, i.e. all five carbon atoms of the cyclopentadienyl unit are coordinated to the ruthenium center. As analyzed previously by us [12a] and others [11e], not all five carbon atoms have the same Ru–C bond lengths. The bond lengths of the two benzenoid carbons are longer compared to the other three carbon atoms of the cyclopentadienyl ring. This can be quantified by

the Δ Ru-C value (here 0.197 and 0.137 Å, respectively), which describes the average difference in bond lengths of the two benzenoid carbon atoms and the other three carbon atoms of the cyclopentadienyl unit [11e,12a,22]. Related complexes exhibit similar Δ Ru-C values around 0.2 Å. The fold angle is the angle between the plane formed by C1-C2-C3 of the C5 ring and by C1-C3-C4-C5 or C1-C3-C4-C9 of two carbon atoms of the C5 ring and the two carbon atoms shared by the C5 ring and the benzenoyl unit; thus, it describes the angle that is formed by the plane of the C5 unit and the benzene unit of the indenyl ligand [11e]. The fold angle takes the value 0 in an ideal η^5 -coordination, and for indenyl complexes, the values typically range below 10°; again, [RuCl(ind)(PPh₃){P(*p*-C₆H₄CF₃)₃}] and [RuCl(ind)(PPh₃){P(3,5-C₆H₃(CF₃)₂)₃}] fall in this range (9.57° and 7.45°, respectively) as do the other two complexes shown in Table 1. An η^3 -coordination would be indicated by a fold angle around 60° [11e].

It has been observed before that the ligand with the strongest *trans* influence will take the position *trans* to the benzo unit of the indenyl ligand [11e]. The *trans* influence weakens the bond strength (and enlarges the bond length) of the two Ru-C bonds of the benzo unit coordinated to the ruthenium. Accordingly, the PPh₃ ligand (as opposed to the fluorinated phosphine ligands) takes the position *trans* to the benzoid portion of the indenylid ligand (schematic structure **A** in in Figure 3). This position provides some evidence that PPh₃ has a larger *trans* influence compared to the fluorinated ligands; however the solid state structures allow only limited conclusions for the situation in solution.

In general, it appears that the placement of electron-withdrawing CF₃ units on the aryl rings in triarylphosphine ligands does not have a profound impact on the Ru-P bond length and other geometric parameters of their respective ruthenium complexes in the solid state when

compared to structurally related ones, such as $[\text{RuCl}(\text{Ind})(\text{PPh}_3)\{\text{P}(\text{pyr})_3\}]$ (Figure 1) and $[\text{RuCl}(\text{Ind})(\text{PPh}_3)_2]$ [7].

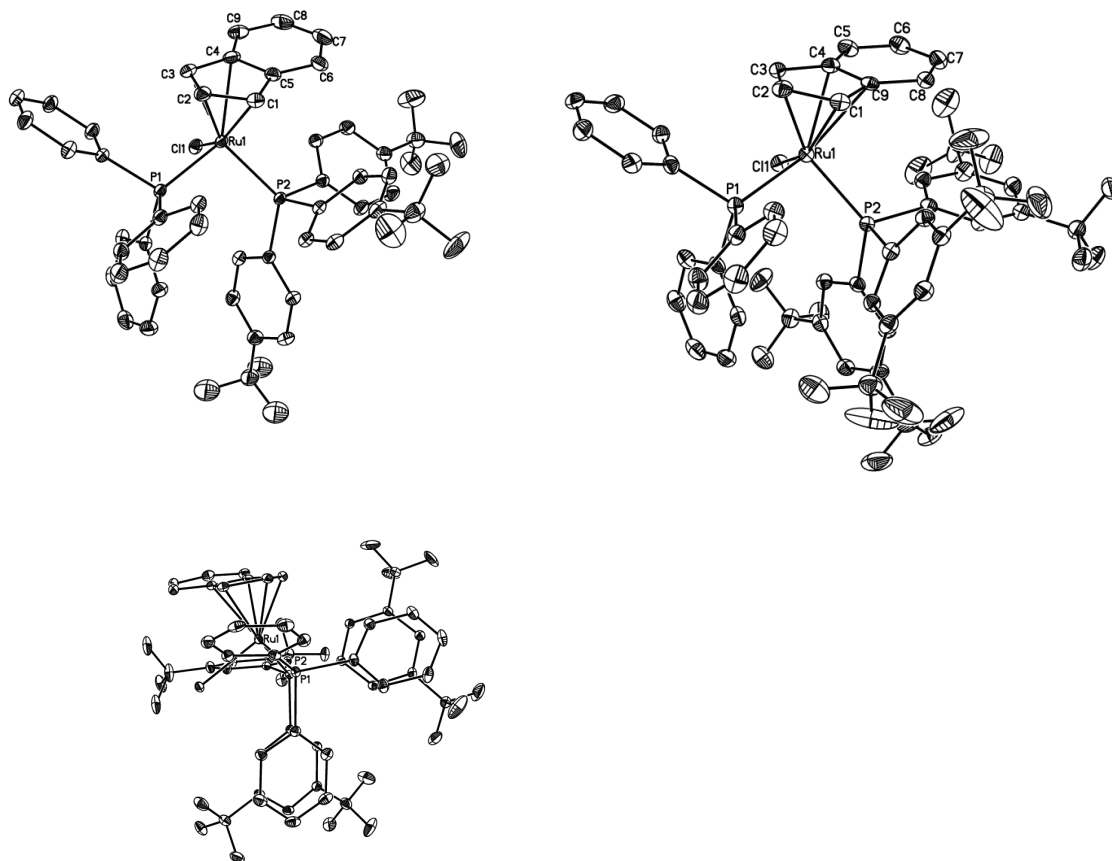


Figure 2. The molecular structures of $[\text{RuCl}(\text{ind})(\text{PPh}_3)\{\text{P}(p\text{-C}_6\text{H}_4\text{CF}_3)_3\}]$ (left) and $[\text{RuCl}(\text{ind})(\text{PPh}_3)\{\text{P}(3,5\text{-C}_6\text{H}_3(\text{CF}_3)_2)_3\}]$ (right and bottom). Hydrogen atoms are omitted for clarity. Crystallographic parameters are given in the experimental, and key bond lengths and angles are listed in Table 1.

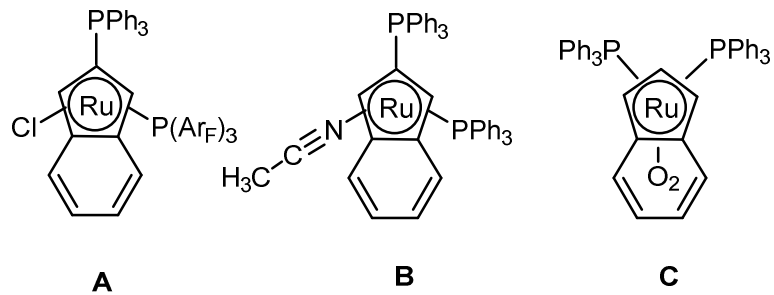


Figure 3. Schematic representation of the position of the indenyl ring in the X-ray structures of indenyl complexes determined in this study. **B** and **C** are discussed later in the text.

Table 1. Selected bond lengths (Å) and angles (°) for complexes of the general formula [RuCl(ind)(PPh₃)PR₃]

	PR ₃ = {P(<i>p</i> -C ₆ H ₄ CF ₃) ₃ }]	PR ₃ ={P(3,5- C ₆ H ₃ (CF ₃) ₂) ₃ }]	PR ₃ =P(pyr) ₃ (Fig. 1) [12a]	PR ₃ =PPh ₃ [20]
<i>Bond lengths</i> (Å)				
Ru-P(1) (PPh ₃)	2.2696(5)	2.2707(9)	2.2323(15)	2.331
Ru-P(2) P(<i>p</i> -C ₆ H ₄ CF ₃) ₃	2.3203(5)	2.2929(9)	2.2760(14)	2.268
Ru-Cl	2.4422(5)	2.4372(8)	2.4362(15)	2.437
<i>Bond Angles</i> (°)				
P(1)-Ru- P(2)	99.585(19)	95.59(3)	97.89(5)	99.21
Cl-Ru- P(1)	92.389(18)	93.03(3)	93.51(5)	92.42
Cl-Ru- P(2)	91.612(17)	95.50(3)	91.79(5)	92.19
<i>Other geometrical parameters</i>				
Ru-C5- ring (Å) ^a	1.904	1.903	1.902	1.918
Δ Ru-C	0.197 ^b	0.137 ^c	0.161	0.221
Fold angle	9.57° ^d	7.45° ^e	7.06°	7.07°

^a Distance between the C5 ring of the indenyl ligand and the ruthenium center.

^b Average difference between the Ru-C1, Ru-C2 and Ru-C3 bond lengths and the Ru-C4 and Ru-C5 bond lengths.

^c Average difference between the Ru-C1, Ru-C2 and Ru-C3 bond lengths and the Ru-C4 and Ru-C9 bond lengths.

^d Angle between the plane formed by C1-C2-C3 and by C1-C3-C4-C5.

^e Angle between the plane formed by C1-C2-C3 and by C1-C3-C4-C9.

2.3. Cyclic Voltammetry

Cyclic voltammetry has been used previously to characterize the electronic properties of ruthenium phosphine complexes by us [12a, 23] and others [24], and we recorded cyclic voltammograms of $[\text{RuCl}(\text{ind})(\text{PPh}_3)\{\text{P}(p\text{-C}_6\text{H}_4\text{CF}_3)_3\}]$ and $[\text{RuCl}(\text{ind})(\text{PPh}_3)\{\text{P}(3,5\text{-C}_6\text{H}_3(\text{CF}_3)_2)_3\}]$. The traces for a scan rate of 0.2 V/s are compiled in Figure 4.

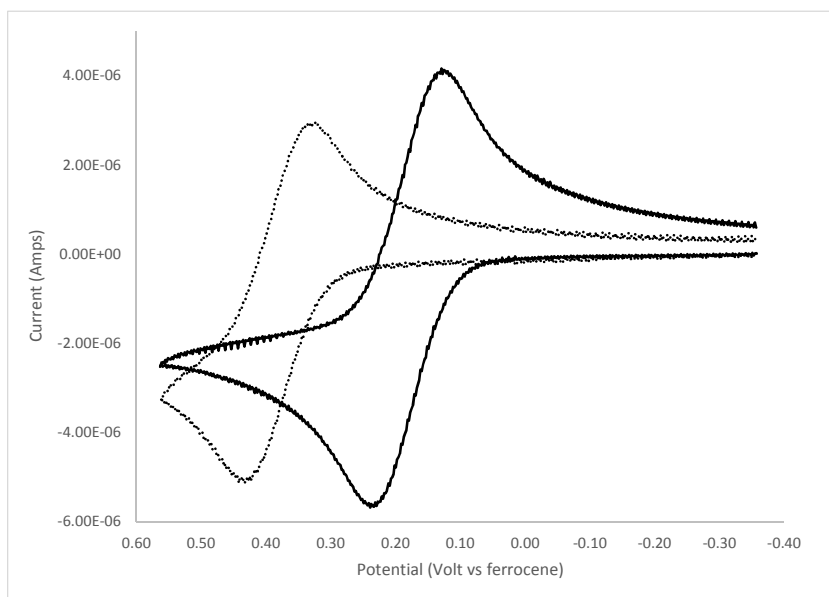


Figure 4. Cyclic voltammetry of ruthenium indenyl complexes in 0.1M $n\text{-Bu}_4\text{PF}_6$ / CH_2Cl_2 , 298K, recorded at a scan rate of 0.2 V/s., $[\text{RuCl}(\text{ind})(\text{PPh}_3)\{\text{P}(p\text{-C}_6\text{H}_4\text{CF}_3)_3\}]$ (0.92 mM concentration, solid line) and $[\text{RuCl}(\text{ind})(\text{PPh}_3)\{\text{P}(3,5\text{-C}_6\text{H}_3(\text{CF}_3)_2)_3\}]$ (0.73 mM concentration, dotted line ...).

The cyclic voltammograms of $[\text{RuCl}(\text{ind})(\text{PPh}_3)\{\text{P}(p\text{-C}_6\text{H}_4\text{CF}_3)_3\}]$ and $[\text{RuCl}(\text{ind})(\text{PPh}_3)\{\text{P}(3,5\text{-C}_6\text{H}_3(\text{CF}_3)_2)_3\}]$ show a high degree of reversibility at different scan rates in that its i_{pc}/i_{pa} values are close to a value of 1 at all scan rates. The E° value for the

oxidation is +0.173 V (vs. $\text{Cp}_2\text{Fe}^{0/+}$, Cp = cyclopentadienyl) and the peak current ratio i_{pc}/i_{pa} is 1.0 at a scan rate of 0.2 V/s for $[\text{RuCl}(\text{ind})(\text{PPh}_3)\{\text{P}(p\text{-C}_6\text{H}_4\text{CF}_3)_3\}]$. For the complex $[\text{RuCl}(\text{ind})(\text{PPh}_3)\{\text{P}(3,5\text{-C}_6\text{H}_3(\text{CF}_3)_2)_3\}]$, the E° value is significantly higher (+0.370 V). The oxidation of $[\text{RuCl}(\text{ind})(\text{PPh}_3)\{\text{P}(3,5\text{-C}_6\text{H}_3(\text{CF}_3)_2)_3\}]$ is also reversible at different scan rates with an i_{pc}/i_{pa} ratio of 0.98 at 0.2 V/s. It appears that the introduction of CF_3 -substituted tris(aryl)phosphine ligands increases the redox potential of the respective complexes compared to the “parent” complex $[\text{RuCl}(\text{ind})(\text{PPh}_3)_2]$ ($E^\circ = -0.023$ V) [12a], which is in line with the higher π -acidic electron-demand of the fluorinated ligands. Interestingly, as determined before in our laboratory, the related complex $[\text{RuCl}(\text{ind})(\text{PPh}_3)\{\text{P}(\text{pyr})_3\}]$ (Figure 1) exhibited a redox potential of +0.34 V. Thus, it appears that the $\text{P}(\text{pyr})_3$ ligand has a π -acidity comparable to that of $\text{P}(3,5\text{-C}_6\text{H}_3(\text{CF}_3)_2)_3$ [12a]

2.4. Catalytic applications

We then investigated the new complexes for their ability to catalytically activate propargylic alcohols [25], and we chose as a test reaction the etherification of propargylic alcohol **1b** with benzyl alcohol **2b** to obtain the propargylic ether **3** (Table 2). We performed preliminary screening reactions with the more easily available precursor complex $[\text{RuCl}(\text{ind})(\text{PPh}_3)_2]$; reactivity trends established in Table 2 were similar to those observed for the new complexes with the fluorinated ligands. The complexes $[\text{RuCl}(\text{ind})(\text{PPh}_3)_2]$, $[\text{RuCl}(\text{ind})(\text{PPh}_3)\{\text{P}(p\text{-C}_6\text{H}_4\text{CF}_3)_3\}]$ and $[\text{RuCl}(\text{ind})(\text{PPh}_3)\{\text{P}(3,5\text{-C}_6\text{H}_3(\text{CF}_3)_2)_3\}]$ themselves did not show catalytic activity for the reaction. However, after activation by chloride abstraction using NaPF_6 , catalytic activity was observed.

Table 2. Screening Reactions

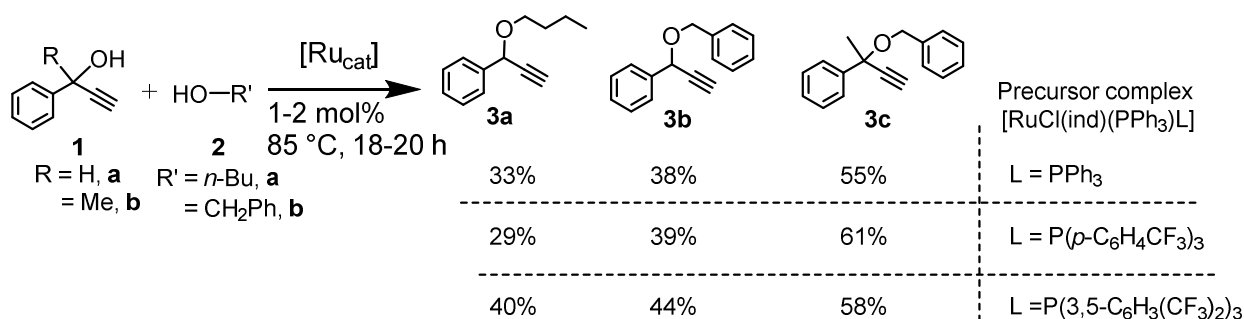
Entry	Solvent	T – t	Catalyst ¹	Activator ²	Results / Products
1	CH ₃ CN / toluene 1:9	80 °C 8 h	[RuCl(ind)(PPh ₃) ₂]	1 equiv. NaPF ₆	no reaction
2	CH ₃ CN / toluene 1:9	80 °C 4 h	[RuCl(ind)(PPh ₃) ₂]	KPF ₆	no reaction
3	CH ₃ CN / toluene 1:9	80 °C 16 h	[RuCl(ind)(PPh ₃) ₂]	NaClO ₄	no reaction
4	CH ₃ CN / toluene 1:9	80 °C 4 h	[RuCl(ind)(PPh ₃) ₂]	6 equiv. NaPF ₆	 80% 20%
5	toluene	80 °C 16 h	[Ru(ind)(MeCN)(PPh ₃) ₂]PF ₆ ³	none	 44 % isolated yield
6	toluene	85 °C 4 h	none	NaPF ₆	 incomplete, only elimination
7	toluene	85 °C 4 h	[Ru(ind)(MeCN)(PPh ₃) ₂]BAR _F ⁴	none	Trace amounts of ether product

¹ 1 – 2 mol%² Number of equivalents for the activator given in relation to the ruthenium catalyst.³ Preformed, chloride-abstracted complex obtained from reaction with NaPF₆, see text.⁴ Preformed, chloride-abstracted complex obtained from reaction with NaBAR_F. BAR_F = Tetrakis(3,5-bis(trifluoromethyl)phenyl)borate, see text.

In general, a high-boiling, aliphatic solvent (such as toluene) was required to observe catalytic activity. However, NaPF₆ is minimally soluble in toluene and we determined that the

addition of a small amount of CH₃CN aided the dissolution of NaPF₆. Accordingly, the best results were obtained, when a 1 : 9 ratio of CH₃CN to toluene in the presence of 4 to 6 equivalents of NaPF₆ (related to the ruthenium catalyst) was employed for the reaction (Table 2, entry 4; one equivalent of NaPF₆ was insufficient, entry 1). Other chloride abstractors such as KPF₆ and NaClO₄ obviously did not activate the ruthenium precursor complex as no reaction was observed (entries 2 and 3), which might be due to the poor solubility in the solvent mixture. NaPF₆ alone gave no etherification product, but resulted in some elimination (entry 6).

Under optimized conditions, the complexes and NaPF₆ were first preheated to 85 °C for 20 minutes in CH₃CN / toluene 1 : 9, followed by addition of the substrates to the preactivated complex. The activated complexes were employed in a number of etherification reactions to give the known [12d] propargylic ethers **3**, and the results are compiled in Scheme 2. All three precursor complexes [RuCl(ind)(PPh₃)₂], [RuCl(ind)(PPh₃){P(*p*-C₆H₄CF₃)₃}] and [RuCl(ind)(PPh₃){P(3,5-C₆H₃(CF₃)₂)₃}] were employed in catalysis (experimental details are given in the Supplementary data), and the yields given in Scheme 2 are for the precursor complexes bearing fluorinated aryl rings. As can be seen, the isolated yields do not significantly differ for the complexes. The isolated yields are moderate; however, the propargylic alcohol and the alcohol nucleophile were employed in almost equimolar amounts. Excess of the alcohol nucleophile over the propargylic alcohol is not required, as sometimes reported for other catalytic systems [25e]. Also, the catalyst load used of 1-2 mol% is lower than that of many other catalyst systems reported in the literature [25e].



Scheme 2. Catalytic application of the new ruthenium complexes

Thus, the activated complexes exhibited catalytic activity, but we could not reach our major goal, i.e. to lower the reaction temperature and to increase the yield of the reactions. In order to improve the catalyst system and to investigate the course of the reaction in greater detail, we performed additional experiments.

2.5. Chloride abstraction products

We first speculated that the chloride abstraction to activate the complexes was inefficient. We, thus, investigated the chloride abstraction by heating the complexes for several hours in presence of NaPF₆ and CH₃CN but without any substrates, and investigated the result by ³¹P{¹H} NMR. The ³¹P{¹H} NMR spectra are shown in Figure 5.

The parent complex [RuCl(ind)(PPh₃)₂] gave a relatively clean (albeit incomplete) reaction to the corresponding acetonitrile complex [Ru(ind)(CH₃CN)(PPh₃)₂]⁺, as indicated by a new ³¹P{¹H} NMR peak at 47.7 ppm (Figure 5, bottom, see also *vide infra* for the independent synthesis of that complex). For the two other complexes [RuCl(ind)(PPh₃){P(*p*-C₆H₄CF₃)₃}] and [RuCl(ind)(PPh₃){P(3,5-C₆H₃(CF₃)₂)₃}] with phosphorylated ligands, the reaction was not as clean (Figure 5, middle and top) and a number of new peaks appeared in the ³¹P{¹H} NMR spectra. For the complex [RuCl(ind)(PPh₃){P(*p*-C₆H₄CF₃)₃}], the starting material was

consumed (Figure 5, middle). Besides a couple of unidentified singlets around 48 ppm, the reaction mixture after chloride abstraction revealed a set of relatively small doublets at 49.3 and 47.4 ppm ($J_{\text{PP}} = 35$ Hz), which was, based on the synthesis of an authentic sample (*vide infra*), attributed to the acetonitrile complex $[\text{Ru}(\text{ind})(\text{CH}_3\text{CN})(\text{PPh}_3)\{\text{P}(p\text{-C}_6\text{H}_4\text{CF}_3)_3\}]^+$. The complex $[\text{RuCl}(\text{ind})(\text{PPh}_3)\{\text{P}(3,5\text{-C}_6\text{H}_3(\text{CF}_3)_2)_3\}]$ gave only partial chloride abstraction, as indicated by corresponding peaks for the starting material in the $^{31}\text{P}\{^1\text{H}\}$ NMR spectrum (Figure 5, top). Only some minor singlets were observed in the spectrum between 47 and 55 ppm. It appears that the more electron-poor complex $[\text{RuCl}(\text{ind})(\text{PPh}_3)\{\text{P}(3,5\text{-C}_6\text{H}_3(\text{CF}_3)_2)_3\}]$ is - compared to the other two complexes - more difficult to ionize.

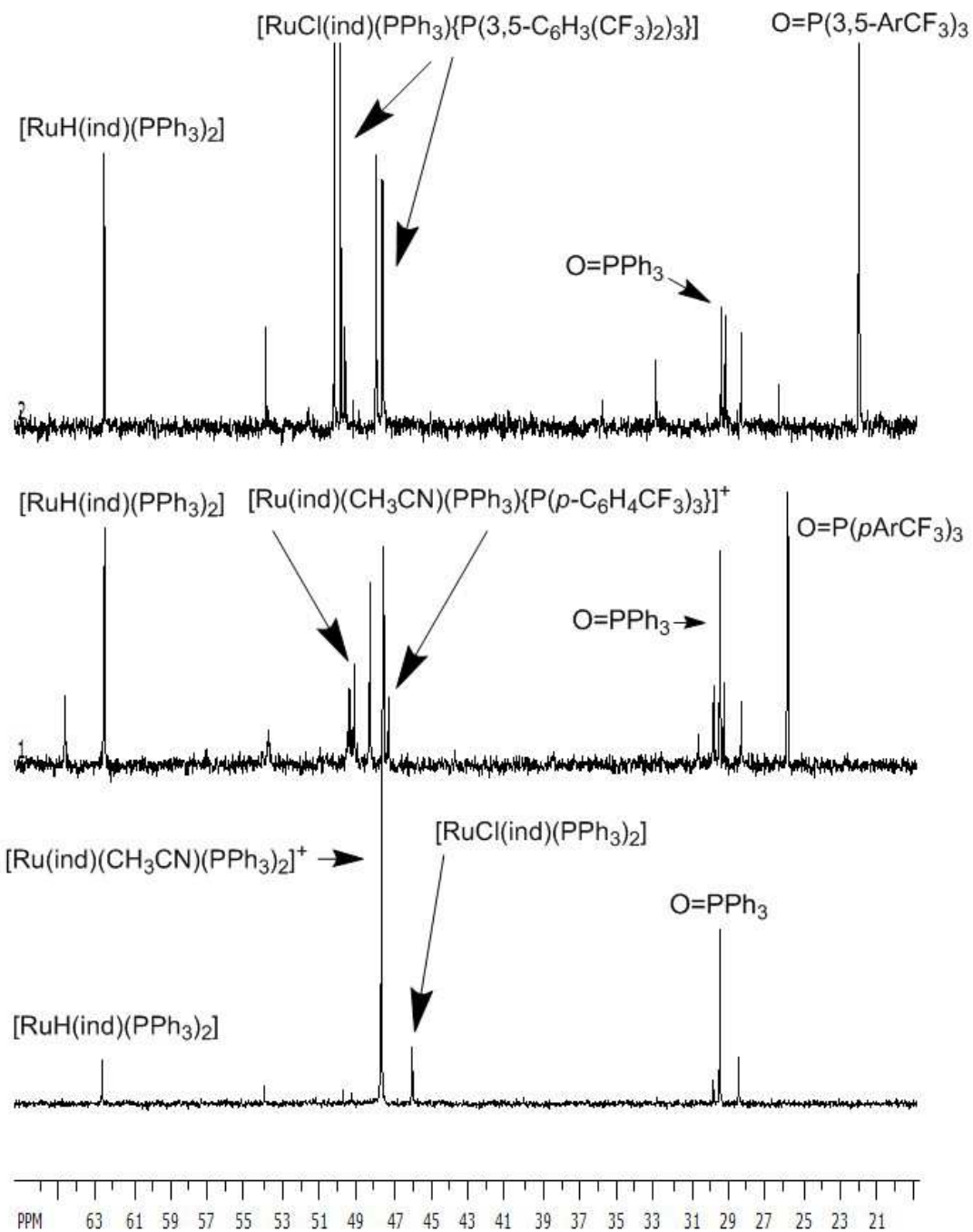


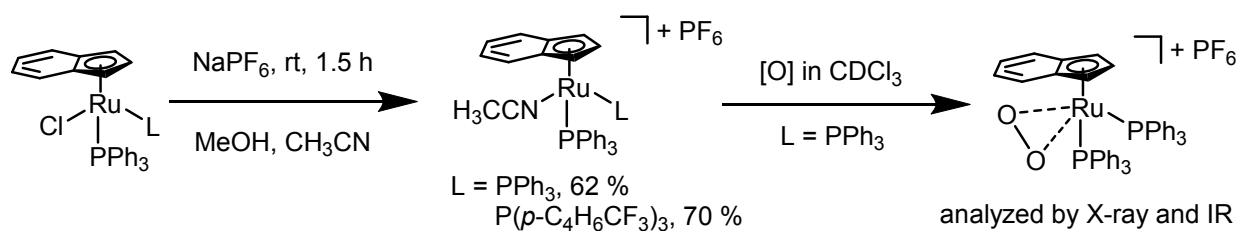
Figure 5. $^{31}P\{^1H\}$ NMR spectra of the complexes $[RuCl(ind)(PPh_3)\{P(3,5-(CF_3)_2C_6H_3)_3\}]$ (top), $[RuCl(ind)(PPh_3)\{P(p-CF_3C_6H_4)_3\}]$ (middle) and $[RuCl(ind)(PPh_3)_2]$ (bottom) after treatment with $NaPF_6$.

For all three complexes, peaks between 21 and 30 ppm indicated the presence of the oxidized ligands O=PPh₃ (29 ppm), O=P(*p*-C₆H₄CF₃)₃ (25.8 ppm) and O=P(3,5-C₆H₃(CF₃)₂)₃ (21.8 ppm). The peak assignments for the latter two phosphine oxides were performed based on NMR experiments, where the corresponding phosphine ligands were oxidized with small amounts of H₂O₂ in CDCl₃ and NMR spectra subsequently recorded.

However, we were intrigued by the fact that the chloride abstraction experiments resulted in a resonance around 63 ppm for all three complexes, indicating the formation of a common species (Figure 5). Furthermore, we observed a peak at -12 ppm in the ¹H NMR spectrum of [RuCl(ind)(PPh₃)₂] after chloride abstraction, pointing towards formation of a hydrido complex. Indeed, comparison with literature values showed that the ¹H and ³¹P{¹H} NMR resonances for the known hydrido complex [RuH(ind)(PPh₃)₂] matches those observed in the reaction mixture after chloride abstraction [7]. Thus, it appeared that the complexes [Ru(ind)(PPh₃){P(*p*-C₆H₄CF₃)₃}]⁺ and [Ru(ind)(PPh₃){P(3,5-C₆H₃(CF₃)₂)₃}]⁺ undergo ligand metathesis to form [Ru(ind)(PPh₃)₂]⁺, which then forms the hydrido complex [RuH(ind)(PPh₃)₂]. It is known that ruthenium complexes can form hydrides in the presence of alcohols or water [26]. In order to determine whether the hydrido complex [RuH(ind)(PPh₃)₂] is the actual catalytically active species in solution, we synthesized the complex independently following a literature procedure [7] and employed it as catalyst in test reactions under the conditions in Scheme 2. Unfortunately, the complex showed no catalytic activity under these conditions. Thus, the formation of the complex [RuH(ind)(PPh₃)₂] constitutes a decomposition pathway of the chloro complexes, resulting potentially in catalyst deactivation.

2.6. Syntheses of Acetonitrile Complexes and their Reactivity

It is known that ruthenium forms stable acetonitrile (CH_3CN) complexes [27]. We next decided to determine whether analytically pure acetonitrile complexes could be employed as catalysts for the title reaction. Accordingly, we synthesized the complex $[\text{Ru}(\text{ind})(\text{CH}_3\text{CN})(\text{PPh}_3)_2] \text{PF}_6$ according to literature procedures for the corresponding known tetrafluoroborate complex $[\text{Ru}(\text{ind})(\text{CH}_3\text{CN})(\text{PPh}_3)_2]^+ \text{BF}_4^-$, as there was no $^{31}\text{P}\{^1\text{H}\}$ NMR spectrum published together with its synthesis (Scheme 3) [28]. The tetrafluoroborate complex has previously been characterized by ^1H NMR and X-ray; for comparison purposes in Figure 5, in addition we analyzed the complex by $^{31}\text{P}\{^1\text{H}\}$ NMR and IR. Following the same procedure, we also synthesized the new acetonitrile complex $[\text{Ru}(\text{ind})(\text{CH}_3\text{CN})(\text{PPh}_3)\{\text{P}(p\text{-C}_6\text{H}_4\text{CF}_3)_3\}] \text{PF}_6$, which was characterized by ^1H and $^{31}\text{P}\{^1\text{H}\}$ NMR and mass spectrometry (Scheme 3). The molecular ion $[\text{Ru}(\text{ind})(\text{CH}_3\text{CN})(\text{PPh}_3)\{\text{P}(p\text{-C}_6\text{H}_4\text{CF}_3)_3\}]^+$ was not observed, but only the fragment $[\text{Ru}(\text{ind})(\text{PPh}_3)\{\text{P}(p\text{-C}_6\text{H}_4\text{CF}_3)_3\}]^+$ which resulted from CH_3CN loss. The fragmentation pattern for the complex and the $^{31}\text{P}\{^1\text{H}\}$ NMR shifts differed from those of $[\text{RuCl}(\text{ind})(\text{PPh}_3)\{\text{P}(p\text{-C}_6\text{H}_4\text{CF}_3)_3\}]$, which provides strong evidence that a new complex had formed. However, we observed a molecular ion for the fragment $[\text{Ru}(\text{ind})(\text{CH}_3\text{CN})(\text{PPh}_3)\{\text{P}(p\text{-C}_6\text{H}_4\text{CF}_3)_3\}]^+$ in the ESI-MS spectrum. Unfortunately, attempts to convert $[\text{RuCl}(\text{ind})(\text{PPh}_3)\{\text{P}(3,5\text{-C}_6\text{H}_3(\text{CF}_3)_2)_3\}]$ to the corresponding acetonitrile complex failed, which could be a consequence of the fact that for this complex chloride abstraction with NaPF_6 is more difficult, as was demonstrated in Figure 5.



Scheme 3. Synthesis of acetonitrile complexes $[\text{Ru}(\text{ind})(\text{CH}_3\text{CN})(\text{PPh}_3)\{\text{L}\}]^+\text{PF}_6^-$.

The complex $[\text{Ru}(\text{ind})(\text{CH}_3\text{CN})(\text{PPh}_3)_2]\text{PF}_6^-$ was also characterized structurally (Figure 6). Selected bond lengths and angles are listed in Table 3. Structural details will be discussed further below. During our characterization efforts for $[\text{Ru}(\text{ind})(\text{CH}_3\text{CN})(\text{PPh}_3)_2]\text{PF}_6^-$ by NMR, we observed the formation of red crystals precipitating out of the CDCl_3 solution in the NMR tube. X-ray analysis revealed that the red crystals are a peroxo complex $[\text{Ru}(\text{ind})(\eta^2\text{-O}_2)(\text{PPh}_3)_2]\text{PF}_6^-$, where O_2 is coordinated as η^2 side-on to the ruthenium center (Scheme 3). A number of ruthenium complexes with η^2 -coordinated O_2 have been structurally characterized [29], and they are typically obtained from a ruthenium precursor complex upon reaction with O_2 . However, attempts to synthesize the complex $[\text{Ru}(\text{ind})(\eta^2\text{-O}_2)(\text{PPh}_3)_2]\text{PF}_6^-$ in bulk failed. Also, analysis of the crystals of $[\text{Ru}(\text{ind})(\eta^2\text{-O}_2)(\text{PPh}_3)_2]\text{PF}_6^-$ by FAB and ESI-MS did not give a molecular ion peak as proof of the coordination (or the presence) of O_2 in the sample. The coordination of O_2 might be reversible, as noted previously by others [29a], making characterization efforts more difficult. However, the IR spectrum of the complex in the solid state exhibited an intense absorption at 828 cm^{-1} ; this absorption is in accordance with η^2 -coordinated O_2 , which typically shows bands between 800 and 900 cm^{-1} [30]. The X-ray data of

[Ru(ind)(η^2 -O₂)(PPh₃)₂]PF₆ together with those of its precursor complex

[Ru(ind)(CH₃CN)(PPh₃)₂]PF₆ are presented in Figure 6 and Table 3.

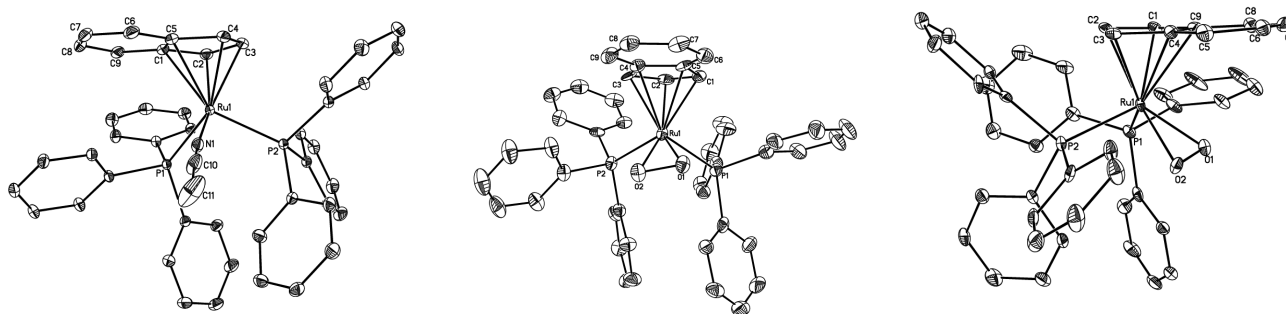


Figure 6. The molecular structures of [Ru(ind)(CH₃CN)(PPh₃)₂]PF₆ (left) and [Ru(ind)(η^2 -O₂)(PPh₃)₂]PF₆ (middle and right). Hydrogen atoms and PF₆⁻ counterions are omitted for clarity. Crystallographic parameters are compiled in the experimental, and key bond lengths and angles are listed in Table 3.

In both complexes the ruthenium centers are slightly distorted octahedra. The acetonitrile complex [Ru(ind)(CH₃CN)(PPh₃)₂]PF₆ is structurally related to the tetrafluoroborate analog previously described in the literature [28]. The bond lengths [2.0436(12) to (2.3913(4) Å)] are comparable to those in the complexes bearing the fluorinated ligands described above despite the fact that the complex is cationic. The bond angles around the ruthenium center in [Ru(ind)(CH₃CN)(PPh₃)₂]PF₆ are also similar except for the P(1)-Ru-P(2) angle, which is larger [103.540(12)°] compared to those of the complexes in Table 1 (all below 100°). The linear CH₃CN ligand is obviously less spatially demanding compared to a Cl, allowing for a larger P(1)-Ru-P(2) angle to better accommodate the bulky PPh₃ ligands coordinated to the ruthenium

center. The parameters corroborating the η^5 -coordination of the indenyl ligand (Δ Ru-C and the fold angle) are similar to those in Table 1, which also holds true for the η^2 -O₂ complex. As discussed above for the other complexes, one of the two PPh₃ ligands takes the position *trans* to the benzoid carbon atoms of the cyclopentadienyl unit of the indenylid ligand (**B** in Figure 3), demonstrating the stronger *trans* influence of PPh₃ compared to CH₃CN.

However, it seems that for the complex [Ru(ind)(η^2 -O₂)(PPh₃)₂PF₆], the bond lengths around the ruthenium center are slightly longer compared to the other complexes. The average Ru-P bond length is slightly longer and the Ru-Cp distance between the ruthenium center and the centroid of the η^5 -coordinated Cp unit of the indenyl ligand is about 0.06 Å longer. The O(1)-O(2) bond length is 1.409(6) Å and, thus, considerably longer compared to the O-O bond length in O₂ (1.21 Å) [30], as expected for side-on coordinated O₂. Similar O-O bond length values have been observed before in metal peroxo complexes [29b], and they lie in between the bond lengths for superoxide (KO₂, 1.28 Å) [30] and peroxide (O₂²⁻, 1.49 Å) [30]. Most interestingly, the η^2 -O₂ ligand is aligned parallel to the indenyl ligand (**C** in Figure 3). Typically, the indenyl ligand occupies an interstitial site between the two phosphine ligands (**A** and **B** in Figure 3).

Table 3. Selected bond lengths (Å) and angles (°)

	[Ru(ind)(CH ₃ CN)(PPh ₃) ₂] ₂ PF ₆	[Ru(ind)(O ₂)(PPh ₃) ₂] ₂ PF ₆
<i>Bond lengths</i> (Å)		
Ru-P(1)	2.3913(4)	2.3415(16)
Ru-P(2)	2.2958(4)	2.3782(17)
Ru-X	2.0436(12) [X = N(1)]	2.003(5) [X = O(1)]
Ru-X	-	2.008(5) [X = O(2)]
O(1)-O(2)	-	1.409(6)
<i>Bond Angles</i> (°)		
P(1)-Ru-P(2)	103.540(12)	96.30(6)
X-Ru-P(1)	93.56(4) [X = N(1)]	81.78(13) [X=O(1)]
O(2)-Ru-P(1)	-	105.38(14)
X-Ru-P(2)	84.87(3) [X=N(1)]	83.86(14) [X=O(2)]
O(1)-Ru-P(2)	-	119.85(14)
O(1)-Ru-O(2)	-	41.13(18)
<i>Other geometrical parameters</i>		
Ru-C5-ring (Å) ^a	1.889	1.952
Δ Ru-C	0.132 ^b	0.204 ^c
Fold angle	6.34° ^d	5.70° ^e

^a Distance between the centroid of the C5 ring of the indenyl ligand and the ruthenium center.

^b Average difference between the Ru-C2, Ru-C3 and Ru-C4 bond lengths and the Ru-C1 and Ru-C5 bond lengths.

^c Average difference between the Ru-C1, Ru-C2 and Ru-C3 and the Ru-C4 and Ru-C5 bond lengths, respectively.

^d Angle between the plane formed by C2-C3-C4 and C1-C2-C4-C5.

^e Angle between the plane formed by C1-C2-C3 and C1-C3-C4-C5.

The X-ray structures demonstrate that in the presence of NaPF₆ and CH₃CN, for [RuCl(ind)(PPh₃)₂] the corresponding acetonitrile complex is obtained. As shown by X-ray and IR, it appears that O₂ from air can replace the CH₃CN ligand to give the corresponding η²-O₂ complex. However, when applied as catalysts in the title reaction under the conditions given in Table 3, only small reactivity or yield differences between [Ru(ind)(CH₃CN)(PPh₃)₂]PF₆ and [Ru(ind)(CH₃CN)(PPh₃){P(*p*-C₆H₄CF₃)₃}]PF₆ and the *in situ* activated complexes were observed (Table 3, entry 5). We, thus, discontinued the investigation of preformed, isolated acetonitrile complex catalysts.

2.7. Comparison of Catalytic Activity

Finally, we speculated whether there were reactivity differences between the three complexes [RuCl(ind)(PPh₃)₂], [RuCl(ind)(PPh₃){P(*p*-C₆H₄CF₃)₃}] and [RuCl(ind)(PPh₃){P(3,5-C₆H₃(CF₃)₂)₃}]. Accordingly, the three precursor complexes were activated by chloride abstraction for a test reaction; product formation was followed over time by NMR. The results are compiled in Figure 7. Somewhat surprisingly, all three precursor complexes gave comparable activities over time, i.e. product formation was comparable over time for the three complexes. This finding reflects the isolated yields for the catalysis products presented in Scheme 2, which are also fairly similar for the three complexes.

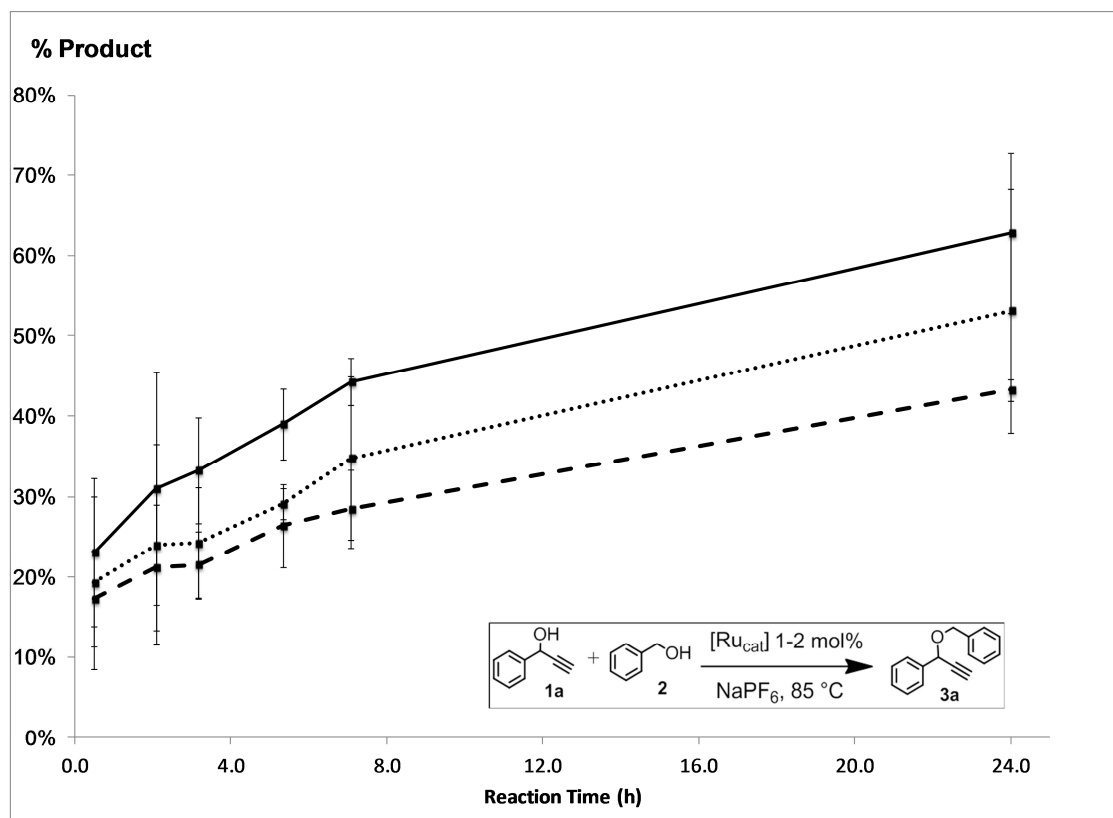


Figure 7. Activity comparison for the ruthenium complexes $[\text{RuCl}(\text{ind})(\text{PPh}_3)\{\text{P}(p\text{-C}_6\text{H}_4\text{CF}_3)_3\}]$ (dotted line) and $[\text{RuCl}(\text{ind})(\text{PPh}_3)\{\text{P}(3,5\text{-C}_6\text{H}_3(\text{CF}_3)_2)_3\}]$ (dashed) after activation by chloride abstraction. The average of three runs for each complex are shown and error bars are given. For comparison, the activity of $[\text{RuCl}(\text{ind})(\text{PPh}_3)_2]$ (solid line) is also included.

While somewhat speculative, the similarities in reactivity point towards a common catalytically active species for all three catalysts appear to be involved. It is known from the literature that the PF_6^- anion can hydrolyze under aqueous conditions [31]. Thus, it cannot be excluded that hydrolysis products of the PF_6^- counter anion or other, common decomposition products of the precursor complexes contribute to the catalytic activity of the system. It appeared

that the chemistry of mixed phosphine complexes of ruthenium of the general formula as in $[\text{RuCl}(\text{ind})(\text{PPh}_3)\{\text{P}(p\text{-C}_6\text{H}_4\text{CF}_3)_3\}]$ and $[\text{RuCl}(\text{ind})(\text{PPh}_3)\{\text{P}(3,5\text{-C}_6\text{H}_3(\text{CF}_3)_2)_3\}]$ is more complex than we originally anticipated (as demonstrated in Figure 5). Further investigations of the catalytic system and about the catalytically active species are ongoing.

3. Conclusion

In conclusion, two new ruthenium complexes of the general formula $[\text{RuCl}(\text{ind})(\text{PPh}_3)\text{L}]$ were synthesized, bearing phosphine ligands L with CF_3 -substituted aryl rings. Structural characterization revealed that the geometry of the new complexes does not differ significantly from related complexes. However, the placement of the fluorinated ligands resulted in increased oxidation potentials compared to the parent complex $[\text{RuCl}(\text{ind})(\text{PPh}_3)_2]$. The new complexes are, after activation through chloride abstraction, catalytically active in the etherification of propargylic alcohols. As investigated through $^{31}\text{P}\{^1\text{H}\}$ NMR, the chloride abstracted fragments $[\text{Ru}(\text{ind})(\text{PPh}_3)\text{L}]^+$ are not very stable and undergo a decomposition reaction in solution, and formation of the hydrido complex $[\text{RuH}(\text{ind})(\text{PPh}_3)_2]$ was observed for the two precursor complexes, indicating ligand metathesis after chloride abstraction. When the catalytic activity of the new complexes $[\text{RuCl}(\text{ind})(\text{PPh}_3)\text{L}]$ was determined for a test reaction and compared to the activity of the parent compound $[\text{RuCl}(\text{ind})(\text{PPh}_3)_2]$, it appeared that all three complexes exhibited similar reactivities. Investigation of the catalytically active species is ongoing.

4. Experimental

4.1. General.

All reactions were carried out under an inert N₂ atmosphere using standard Schlenk techniques. The ligands tris(4-(trifluoromethyl)phenyl)phosphine, P(*p*-C₆H₄CF₃)₃, and tris(3,5-bis(trifluoromethyl)phenyl)phosphine, P(3,5-C₆H₃(CF₃)₂)₃, were purchased from Strem Chemicals and used as is. All other chemicals, including NaPF₆, were used as supplied from Sigma-Aldrich unless otherwise noted and used as received. The complex [RuCl(ind)(PPh₃)₂] was synthesized following the literature [7]. THF was distilled from Na/benzophenone under N₂. Ethyl acetate, hexane, toluene, CH₂Cl₂, and ClCH₂CH₂Cl were distilled prior to use; solvents used in catalysis were used as is.

4.2. Instruments and measurements

NMR spectra for characterization were collected at room temperature on a Varian Unity 300 MHz or Bruker Avance 300 MHz instrument; all chemical shifts (δ) are reported in ppm and are referenced to a residual solvent signal. IR spectra were collected on a Thermo Nicolet 360 FT-IR spectrometer. FAB and exact mass data were collected on a JEOL MStation [JMS-700] Mass Spectrometer. Melting points were determined on a Thomas Hoover uni-melt capillary melting point apparatus and are uncorrected. Elemental analyses were performed by Atlantic Microlab Inc., Norcross, GA, USA.

4.3. [RuCl(ind)(PPh₃){P(*p*-C₆H₄CF₃)₃}]

A Schlenk flask containing [RuCl(ind)(PPh₃)₂] (0.260 g, 0.335 mmol), P(*p*-C₆H₄CF₃)₃ (0.158 g, 0.339 mmol), and THF (5 mL) was refluxed gently for 4 hours under nitrogen. The

solvent was removed via vacuum. The complex was isolated as a red solid (0.148 g, 0.125 mmol, 57 %) by column chromatography, silica gel (2×10 cm) using CH₂Cl₂ and petroleum ether (1:3) as eluent. The product was recrystallized from CH₂Cl₂ layered with hexanes. m.p. 122-124 °C (dec., capillary). ¹H NMR (300 MHz, CDCl₃) δ 7.40-7.29 (m, 24H, arom.), 7.20-7.11 (m, 6H, arom.), 6.92-6.81 (m, 2H, arom.), 4.73-4.70 (m, 1H, indenyl), 4.43 (br s, 1H, indenyl), 3.74 (s, 1H, indenyl); ¹³C{¹H} NMR (75 MHz, CDCl₃) δ 140.7 (s), 140.2 (s), 136.6 (s), 136.0 (s), 134.2 (s), 134.1 (s), 133.8 (s), 133.6 (s), 131.6 (s), 131.2 (s), 130.8 (s), 130.3 (s), 129.7 (s), 129.4 (s), 129.0 (s), 128.6 (s), 127.8 (s), 127.7 (s), 125.8 (s), 125.5 (s), 124.7 (m), 123.4 (s), 122.2 (s), 118.6 (s), 112.8 (s), 112.7 (s), 110.6 (br s), 89.6 (s), 70.9 (s), 70.8 (s), 64.8 (s), 53.7 (s, CH₂Cl₂), 31.8 (s, hexanes), 22.9 (s, hexanes), 14.4 (s, hexanes); ³¹P{¹H} NMR (121 MHz, CDCl₃) δ 50.1 (d, *J*_{PP}=42 Hz), 44.2 (d, *J*_{PP}=42 Hz); ¹⁹F{¹H} NMR (282 MHz, CDCl₃) δ -62.9. IR (neat, solid): $\tilde{\nu}$ = 3041 (w), 2956 (w), 2923 (w), 1604 (w), 1479 (w), 1395 (w), 1317 (w), 1162 (w), 1113 (w), 1085 (s), 1055 (s), 1012 (s), 842 (m), 823 (m), 778 (m), 746 (m) cm⁻¹. FAB-MS *m/z* (%) 718 (20) [RuCl(ind){P(*p*-C₆H₄CF₃)₃}]⁺, 683 (22) [Ru(ind){P(*p*-C₆H₄CF₃)₃}]⁺, 483 (32) [O=P(*p*-C₆H₄CF₃)₃]⁺, 466 (100) [P(*p*-C₆H₄CF₃)₃]⁺, 321 (15) [P(*p*-C₆H₄CF₃)₂]⁺, 262 (43) [PPh₃]⁺. C₄₈H₃₄ClF₉P₂Ru (980.24): calcd. C 58.81, H 3.50; found C 59.19, H 3.89.

4.4. [RuCl(ind)(PPh₃){P(3,5-C₆H₃(CF₃)₂)₃}]

A Schlenk flask containing [RuCl(ind)(PPh₃)₂] (0.171 g, 0.219 mmol), P(3,5-C₆H₃(CF₃)₂)₃ (0.165 g, 0.242 mmol), and THF (5 mL) was refluxed gently for 4 hours under nitrogen. The solvent was removed via vacuum. The complex was isolated as a red solid (0.077 g, 0.079 mmol, 24 %) by column chromatography, silica gel (2 × 10 cm) using CH₂Cl₂ and petroleum ether (1:3 /

v:v) as eluent. The complex was recrystallized from CH₂Cl₂ layered with hexanes, mp 141-143 °C (dec., capillary). ¹H NMR (300 MHz, CDCl₃) δ 7.89-7.85 (m, 9H, arom.), 7.39-7.27 (m, 10H, arom.), 7.19-7.14 (m, 6H, arom.), 6.95-6.92 (m, 1H, arom.), 6.59-6.55 (m, 2H, arom.), 5.15 (br s, 1H, indenyl), 4.84 (m, 1H, indenyl), 3.82 (s, 1H, indenyl) ; ¹³C{¹H} NMR (75 MHz, CDCl₃) δ 138.3 (s), 137.8 (s), 136.5 (s), 135.9 (s), 133.5 (d, *J*_{CP}=9.7 Hz), 133.3 (m), 131.8 (d, *J*_{CP}=9.1 Hz), 131.4 (d, *J*_{CP}=9.1 Hz), 129.9 (s), 129.3 (s), 128.0 (d, *J*_{CP}=9.7 Hz), 126.7 (s), 124.8 (s), 123.9 (s), 121.1 (s), 111.0 (s), 109.4 (s), 91.9 (s), 75.9 (s), 75.8 (s), 63.3 (s), 53.7 (s, CH₂Cl₂) ; ³¹P{¹H} NMR (121 MHz, CDCl₃) δ 50.1 (d, *J*_{PP}=42 Hz), 47.8 (d, *J*_{PP}=42 Hz); ¹⁹F{¹H} NMR (282 MHz, CDCl₃) δ -62.8. IR (neat, solid): $\tilde{\nu}$ = 3053 (w), 3022 (w), 2308 (w), 2117 (w), 1888 (w), 1821 (w), 1614 (w), 1478 (w), 1432 (w), 1351 (s), 1275 (s), 1176 (m), 1117 (s), 1088 (s), 893 (m), 843 (m), 816 (m), 748 (m) cm⁻¹. HRMS: calcd. for C₅₁H₃₁F₁₈P₂¹⁰²Ru 1149.0657; found 1149.047. C₅₁H₃₁ClF₁₈P₂Ru (1184.23): calcd. C 51.73, H 2.64; found C 50.72, H 2.70.

4.5. [Ru(ind)(CH₃CN)(PPh₃)₂]PF₆

A Schlenk flask containing [RuCl(ind)(PPh₃)₂] (0.311 g, 0.401 mmol), NaPF₆ (0.070 g, 0.417 mmol), CH₃CN (0.200 mL, 3.829 mmol), and MeOH (15 mL) was refluxed gently for 4 hours under nitrogen. An orange precipitate formed. The precipitate was isolated by vacuum filtration and dried under high vacuum to give the product as an orange solid (0.230 g, 0.248 mmol, 62 %). ¹H NMR (300 MHz, CDCl₃) δ 7.29-7.21 (m, 20H, arom.), 7.18-7.12 (m, 14H, arom.), 6.88-6.80 (m, 14H, arom.), 4.66 (br s, 1H, indenyl), 4.42 (s, 2H, indenyl), 2.12 (s, 3H, CH₃CN); ³¹P{¹H} NMR (121 MHz, CDCl₃) δ 47.7 (s), -146.0 (septet, *J*_{FP}=712 Hz, PF₆⁻). IR (neat, solid): $\tilde{\nu}$ = 3637 (w), 3322 (w), 3049 (w), 2278 (w), 1626 (w), 1582 (w), 1531 (w), 1478 (m),

1431 (m), 1329 (w), 1187 (w), 1156 (w), 1088 (w), 1026 (w), 996 (w), 829 (s), 755 (s), 746 (s) cm^{-1} . FAB-MS m/z (%) 741 (80) $[\text{Ru}(\text{ind})(\text{PPh}_3)_2]^+$, 479 (100) $[\text{Ru}(\text{ind})(\text{PPh}_3)]^+$. ESI-MS m/z (%) 782 (20) $[\text{Ru}(\text{ind})(\text{CH}_3\text{CN})(\text{PPh}_3)_2]^+$, 741 (100) $[\text{Ru}(\text{ind})(\text{PPh}_3)_2]^+$.

4.6. $[\text{Ru}(\text{ind})(\text{CH}_3\text{CN})(\text{PPh}_3)\{\text{P}(p\text{-C}_6\text{H}_4\text{CF}_3)_3\}]\text{PF}_6$

A Schlenk flask containing $[\text{RuCl}(\text{ind})(\text{PPh}_3)\{\text{P}(p\text{-C}_6\text{H}_4\text{CF}_3)_3\}]$ (0.042 g, 0.043 mmol), NaPF_6 (0.008 g, 0.050 mmol), CH_3CN (0.200 mL, 3.829 mmol), and MeOH (10 mL) was stirred at room temperature for 1.5 hours under nitrogen. The solvent was removed and solids were washed with diethyl ether and dried. The residue was passed through a cotton-filled pipette using chloroform. The residue was dried and the product was isolated as a yellow-orange solid (0.034 g, 0.030 mmol, 69.9 %). ^1H NMR (300 MHz, CDCl_3) δ 7.29-7.21 (m, 20H, arom.), 7.18-7.12 (m, 14H, arom.), 6.88-6.80 (m, 14H, arom.), 4.66 (br s, 1H, indenyl), 4.42 (s, 2H, indenyl), 2.12 (s, 3H, CH_3CN); $^{31}\text{P}\{^1\text{H}\}$ NMR (121 MHz, CDCl_3) δ 49.5 (d, $J_{\text{PP}}=35$ Hz), 47.4 (d, $J_{\text{PP}}=35$ Hz), -141.0 (septet, $J_{\text{FP}}=712$ Hz, PF_6^-). IR (neat, solid): $\tilde{\nu}$ = 3069 (w), 2930 (w), 2864 (w), 2320 (w), 1604 (w), 1478 (w), 1433 (w), 1394 (w), 1318 (s), 1165 (m), 1120 (s), 1088 (m), 1056 (s), 1012 (m), 824 (s), 745 (m). FAB-MS m/z (%) 945 (70) $[\text{Ru}(\text{ind})\{\text{P}(p\text{-C}_6\text{H}_4\text{CF}_3)_3\}(\text{PPh}_3)]^+$, 683 (40) $[\text{Ru}(\text{ind})\{\text{P}(p\text{-C}_6\text{H}_4\text{CF}_3)_3\}]^+$, 479 (100) $[\text{Ru}(\text{ind})(\text{PPh}_3)]^+$. ESI-MS m/z (%) 986 (25) $[\text{Ru}(\text{ind})(\text{CH}_3\text{CN})(\text{PPh}_3)\{\text{P}(p\text{-C}_6\text{H}_4\text{CF}_3)_3\}]^+$, 945 (100) $[\text{Ru}(\text{Indenyl})(\text{PPh}_3)(\text{P}(\text{ArCF}_3)_3)]^+$.

4.7. $[\text{Ru}(\text{ind})(\eta^2\text{-O}_2)(\text{PPh}_3)_2]\text{PF}_6$

A NMR tube containing $[\text{Ru}(\text{ind})(\text{CH}_3\text{CN})(\text{PPh}_3)_2]\text{PF}_6$ in CDCl_3 was allowed to rest on the bench top for 72 hours, over which dark solid crystals deposited. IR (neat, solid): $\tilde{\nu}$ = 3056 (w),

2920 (m), 2850 (w), 2283 (w), 1479 (m), 1432 (m), 1186 (w), 1087 (m), 996 (w), 909 (m), 828 (s, $\eta^2\text{-O}_2$), 723 (s) cm^{-1} . From X-ray sample (in Nujol): FAB-MS m/z (%) 741 (52) $[\text{Ru}(\text{ind})(\text{PPh}_3)_2]^+$, 625 (10) $[\text{Ru}(\text{PPh}_3)_2]^+$, 479 (100) $[\text{Ru}(\text{ind})(\text{PPh}_3)]^+$, 363 (16) $[\text{Ru}(\text{PPh}_3)]$, 279 (64) $[\text{O}=\text{PPh}_3]$. From separate crystal: ESI-MS m/z (%) 782 $[\text{Ru}(\text{ind})(\text{CH}_3\text{CN})(\text{PPh}_3)_2]^+$, 741 $[\text{Ru}(\text{ind})(\text{PPh}_3)_2]^+$.

4.8 Catalysis

Unless otherwise indicated, the ruthenium complexes were placed into a screw-capped vial containing 1 mL of acetonitrile in toluene (1 MeCN: 9 Tol), and NaPF_6 (4 molar equivalents with respect to ruthenium), and heated for approximately 20 minutes. To this solution, the propargyl alcohol and substituent nucleophile were added and allowed to heat for the remainder of the reaction time.

4.9. Activity determinations in Figure 7

The respective precursor complex (0.0061 mmol, 2 mol %) was placed into an NMR tube along with NaPF_6 (0.006 g, 0.036 mmol) and CH_3CN (0.02 mL). The mixture was heated for 5 minutes at 85 °C. A solution containing 1-phenyl-2-propyn-1-ol (**1a**, 0.041 g, 0.31 mmol), benzyl alcohol (**2b**, 42 mg, 0.39 mmol) and *p*-dimethoxybenzene (internal standard, 0.002 g) in toluene- d_8 (0.6 mL) was added to each NMR tube. The mixture was heated at 85 °C for 24 hours, where ^1H NMR spectra were recorded for each reaction mixture over a consistent time period. Integration of the diastereotopic doublets at δ 4.78 (d, $J_{\text{HH}}=11.7\text{Hz}$, CH_2 , 2H) for the

product in the spectrum were referenced to the aromatic protons of *p*-dimethoxybenzene at δ 6.71 (4H).

4.10. Cyclic Voltammetry

Voltammograms were recorded in a three-electrode BAS electrochemical cell in a Vacuum Atmospheres HE-493 drybox under an atmosphere of argon in 0.1M NBu₄PF₆ / CH₂Cl₂ at 298 K. A 1.6 mm Pt disk electrode was used as the working electrode, a platinum wire was used as the auxiliary electrode, and a silver wire was used a pseudo-reference electrode. Potentials were calibrated against the Cp*₂Fe^{0/+} couple, which is known to occur at -0.548V vs the Cp₂Fe^{0/+} couple for this solvent medium [32]. The potentials in this paper can be changed to SCE reference values by addition of 0.56 V. Voltammograms were collected at 0.05 – 1.6 V/s with an EG&G PAR 263A potentiostat interfaced to a computer operated with EG&G PAR Model 270 software.

4.11. X-ray Structure Determination for [RuCl(ind)(PPh₃){P(*p*-C₆H₄CF₃)₃}],

[RuCl(ind)(PPh₃){P(3,5-C₆H₃(CF₃)₂)₃}], [Ru(ind)(CH₃CN)(PPh₃)₂]]PF₆ and [Ru(ind)(η^2 -O₂)(PPh₃)₂]]PF₆

Crystals of [RuCl(ind)(PPh₃){P(*p*-C₆H₄CF₃)₃}], [RuCl(ind)(PPh₃){P(3,5-C₆H₃(CF₃)₂)₃}], [Ru(ind)(CH₃CN)(PPh₃)₂]]PF₆ of appropriate dimension were obtained by diffusion of CH₂Cl₂ into hexane solutions of the complexes. Crystals of [Ru(ind)(η^2 -O₂)(PPh₃)₂]]PF₆ were obtained by storage of a CDCl₃ solution of [Ru(ind)(CH₃CN)(PPh₃)₂]]PF₆ under aerobic conditions and directly taken from the reaction mixture. Crystals of approximate

dimensions were mounted on MiTeGen cryoloops in random orientations. Preliminary examination and data collection were performed using a Bruker X8 Kappa Apex II Charge Coupled Device (CCD) Detector system single crystal X-ray diffractometer equipped with an Oxford Cryostream LT device. All data were collected using graphite monochromated Mo K α radiation ($\lambda = 0.71073 \text{ \AA}$) from a fine focus sealed tube X-ray source. Preliminary unit cell constants were determined with a set of 36 narrow frame scans. Typical data sets consist of combinations of ω and Φ scan frames with typical scan width of 0.5° and counting time of 15 seconds/frame at a crystal to detector distance of 4.0 cm. The collected frames were integrated using an orientation matrix determined from the narrow frame scans. Apex II and SAINT software packages [33] were used for data collection and data integration. Analysis of the integrated data did not show any decay. Final cell constants were determined by global refinement of reflections harvested from the complete data set. Collected data were corrected for systematic errors using SADABS [33] based on the Laue symmetry using equivalent reflections.

Crystal data and intensity data collection parameters are listed in Table 4. Structure solution and refinement were carried out using the SHELXTL- PLUS software package [34]. The structures were solved and refined successfully in the space groups $P2_1$ for $[\text{Ru}(\text{ind})(\text{CH}_3\text{CN})(\text{PPh}_3)_2]\text{PF}_6$ and $P-1$ for all other complexes. Full matrix least-squares refinements were carried out by minimizing $\sum w(F_o^2 - F_c^2)^2$. The non-hydrogen atoms were refined anisotropically to convergence. All hydrogen atoms were treated using appropriate riding model (AFIX m3). The final residual values and structure refinement parameters are listed in Table 4.

Table 4. Crystallographic Parameters

	[RuCl(ind)(PPh ₃)(P(<i>p</i> -C ₆ H ₄ CF ₃) ₃)]	[RuCl(ind)(PPh ₃){P(3,5-C ₆ H ₃ (CF ₃) ₂) ₃ }]	[Ru(ind)(CH ₃ CN)(PPh ₃) ₂]PF ₆	[Ru(ind)(η ² -O ₂)(PPh ₃) ₂]PF ₆
Empirical formula	(C ₄₈ H ₃₄ ClF ₉ P ₂ Ru) ₂ (CHCl ₃) ₃	(C ₅₁ H ₃₁ ClF ₁₈ P ₂ Ru) ₂ Et ₂ O	C ₄₇ H ₄₀ F ₆ NP ₃ Ru	C ₄₅ H ₃₇ F ₆ O ₂ P ₃ Ru
Formula weight	2318.52	2456.54	926.78	917.72
Temperature K / Wavelength Å	100(2) / 0.71073	100(2) / 0.71073	100(2) / 0.71073	100(2) K / 0.71073
Crystal system	Triclinic	Triclinic	Monoclinic	Triclinic
Space group	P-1	P-1	P2 ₁	P-1
Unit cell dimensions	a = 9.5521(3) Å b = 11.5438(4) Å c = 21.3297(8) Å α = 90.0613(19)° β = 90.123(2)° γ = 90.9485(18)°	a = 11.3198(4) Å b = 20.1160(10) Å c = 22.2959(10) Å α = 101.841(2)° β = 93.1865(18)° γ = 94.4486(19)°	a = 10.5101(13) Å b = 17.3270(19) Å c = 11.2487(13) Å α = 90° β = 96.677(7)° γ = 90°	a = 9.8032(5) Å b = 14.8889(8) Å c = 19.5349(10) Å α = 72.190(3)° β = 79.428(3)° γ = 71.868(3)°
Volume / Z	2351.64(14) Å ³ / 1	4940.7(4) Å ³ / 2	2034.6(4) Å ³ / 2	2567.5(2) Å ³ / 2
Density (calculated)	1.637 Mg/m ³	1.651 Mg/m ³	1.531 Mg/m ³	1.187 Mg/m ³
Absorption coefficient	0.786 mm ⁻¹	0.545 mm ⁻¹	0.567 mm ⁻¹	0.451 mm ⁻¹
F(000)	1162	2456	944	932
Crystal size / mm ³	0.499 x 0.348 x 0.337	0.406 x 0.337 x 0.189	0.598 x 0.365 x 0.219	0.384 x 0.199 x 0.107
Theta range for data collection	1.764 to 37.238°	0.936 to 27.799°	1.823 to 40.516°	1.100 to 26.492°
Index ranges	-16 ≤ h ≤ 16, -17 ≤ k ≤ 19, -36 ≤ l ≤ 36	-14 ≤ h ≤ 14, -26 ≤ k ≤ 25, 0 ≤ l ≤ 29	-18 ≤ h ≤ 19, -28 ≤ k ≤ 30, -20 ≤ l ≤ 19	-9 ≤ h ≤ 12, -18 ≤ k ≤ 18, -24 ≤ l ≤ 24
Reflections collected	59057	22976	92778	39837
Independent reflections	59057 [R(int) = 0.018]	22976 [R(int) = 0.042]	24235 [R(int) = 0.028]	10242 [R(int) = 0.070]
Absorption correction	Semi-empirical from equivalents	Semi-empirical from equivalents	Semi-empirical from equivalents	Semi-empirical from equivalents
Max. and min. transmission	0.791035 and 0.737117	0.862066 and 0.748420	0.7693 and 0.7103	0.7672 and 0.6547
Data / restraints / parameters	59057 / 37 / 624	22976 / 343 / 1392	24235 / 1 / 523	10242 / 73 / 545
Goodness-of-fit on F ²	1.058	1.011	1.053	1.044
Final R indices [I > 2σ(I)]	R1 = 0.0497,	R1 = 0.0499,	R1 = 0.0236,	R1 = 0.0788,
R indices (all data)	wR2 = 0.1341	wR2 = 0.1289	wR2 = 0.0530	wR2 = 0.1803
Largest diff. peak and hole / e.Å ⁻³	2.245 and -1.603	1.617 and -0.837	0.763 and -0.551	1.356 and -1.905

Absolute structure determination was carried out using Parson's method [35] for [Ru(ind)(CH₃CN)(PPh₃)₂]]PF₆ with Flack $x = -0.021(4)$ from 10263 selected quotients.

For the compound [Ru(ind)(η^2 -O₂)(PPh₃)₂]]PF₆ Platon-Squeeze [36] was used to remove badly disordered solvent molecules (3 \times CHCl₃) The counter ion PF₆ is also disordered and the disorder was resolved with partial occupancy F atoms with geometrical restraints.

For the complex [RuCl(ind)(PPh₃){P(*p*-C₆H₄CF₃)₃}], half a molecule of ethylacetate was found in the lattice. Two CF₃ groups and the CH₃ of the solvent were disordered. The disorder was modeled with partial occupancy atoms and geometrical restraints.

The data for [RuCl(ind)(PPh₃){P(3,5-C₆H₃(CF₃)₂)₃}] was twinned. A two component twin model was used for refinement with BASF = 0.49. 1.5 molecules of CHCl₃/Ru were found in the lattice. Disordered CF₃ group was refined with partial occupancy F atoms with geometrical restraints.

Tables of calculated and observed structure factors are available in electronic format.

Appendix A. Supplementary data.

Crystallographic data for the structural analysis has been deposited with the Cambridge Crystallographic Data Centre, CCDC No. 1518190 for complex [RuCl(ind)(PPh₃){P(*p*-C₆H₄CF₃)₃}], CCDC No. 1518189 for complex [RuCl(ind)(PPh₃){P(3,5-C₆H₃(CF₃)₂)₃}], CCDC No. 1518188 for complex [Ru(ind)(CH₃CN)(PPh₃)₂]]PF₆ and CCDC No. 1518187 for complex [Ru(ind)(η^2 -O₂)(PPh₃)₂]]PF₆. Copies of this information may be obtained free of charge via <http://www.ccdc.cam.ac.uk>. Supplementary data [experimental details for the known catalysis products in Scheme 2, NMR spectra (¹H, ¹³C{¹H}, ³¹P{¹H})] for the metal complexes

[RuCl(ind)(PPh₃){P(*p*-C₆H₄CF₃)₃}] and [RuCl(ind)(PPh₃){P(3,5-C₆H₃(CF₃)₂)₃}] and all catalysis products] can be found at xxx.

Acknowledgments

We would like to thank the National Science Foundation (NSF CHE-1300818, EBB; CHE-156509, MJS) for financial support. Further funding from the National Science Foundation for the purchase of the NMR spectrometer (CHE-9974801), the ApexII diffractometer (MRI, CHE-0420497), and the mass spectrometer (CHE-9708640) is acknowledged.

References

[1] (a) I. Dragutan, V. Dragutan, A. Demonceau, *Molecules* 20 (2015)17244–17274; (b) P. Kumar, R. Kumar Gupta, D. Shankar Pandey, *Chem. Soc. Rev.* 43 (2014) 707–733; (c) F. Nicks, Y. Borguet, S. Delfosse, D. Bicchielli, L. Delaude, X. Sauvage, A. Demonceau, *Aust. J. Chem.* 62 (2009) 184–207; (d) C. Bonaccorsi, A. Mezzetti, *Curr. Org. Chem.* 10 (2006) 225–240; (e) K. Grela, A. Michrowska, M. Bieniek, *The Chemical Record* 6 (2006) 144–156; f) H. Schaffrath, W. Keim, *J. Mol. Catal. A* 168 (2001) 9–14.

[2] S.-I. Murahashi, D. Zhang, *Chem. Soc. Rev.* 37 (2008) 1490–1501.

[3] (a) D. J. Nelson, S. Manzini, C. A. Urbina-Blanco, S. P. Nolan, *Chem. Commun.* 50 (2014) 10355–10375; (b) Y. Vidavsky, A. Anaby, N. G. Lemcoff, *Dalton Trans.* 41 (2012) 32–43; (c) K. Bieger, J. Díez, M. Pilar Gamasa, J. Gimeno, M. Pavlišta, Y. Rodríguez-Álvarez, S. García-Granda, R. Santiago-García, *Eur. J. Inorg. Chem.* (2002) 1647–1656; (d) R. H. Grubbs, *Tetrahedron* 60 (2004) 7117–7140.

[4] (a) J. Francos, S. E. García-Garrido, J. García-Álvarez, P. Crochet, J. Gimeno, V. Cadierno, *Inorg. Chim. Acta* 455 (2017) 398–414; (b) C. Chen, F. Verpoort, Q. Wu, *RSC Adv.* 6 (2016) 55599–55607; (c) J. M. Sears, W.-C. Lee, B. J. Frost *Inorg. Chim. Acta* 431 (2015) 248–257; (d) V. S. Thirunavukkarasu, S. I. Kozhushkov, L. Ackermann, *Chem. Commun.* 50 (2014) 29–39; (e) P. Crochet, V. Cadierno, *Top. Organomet. Chem.* 48 (2014) 48: 81–118; (f) J. Moran, M. J. Krische, *Pure Appl. Chem.* 84 (2012) 1729–1739.

[5] (a) A. A. Nazarov, C. G. Hartinger, P. J. Dyson, *J. Organomet. Chem.* 751 (2014) 251–260; (b) M. I. Webb, B. Wu, T. Jang, R. A. Chard, E. W. Y. Wong, M. Q. Wong, D. T. T. Yapp, C. J. Walsby, *Chem. Eur. J.* 19 (2013) 17031–17042; (c) O. Mazuryk, K. Kurpiewska, K. Lewiński, G. Stochel, M. Brindell, *J. Inorg. Biochem.* 116 (2012) 11–18; (d) N. P. E. Barry, P. J. Sadler, *Chem. Soc. Rev.* 41 (2012) 3264–3279; (e) Y. K. Yan, M. Melchart, A. Habtemariam, P. J. Sadler, *Chem. Commun.* (2005) 4764–4776.

[6] (a) J. M. Cole, K. Y. M. Yeung, G. Pace, S. O. Sylvester, D. Mersch, R. H. Friend, *CrystEngComm* 17 (2015) 5026–5031; (b) A. Breivogel, C. Kreitner, K. Heinze, *Eur. J. Inorg. Chem.* (2014) 5468–5490; (c) S. Fantacci, F. De Angelis, *Coord. Chem. Rev.* 255 (2011) 2704–2726.

[7] L. A. Oro, M. A. Ciriano, M. Campo, C. Foces-Foces, F. H. J. Cano, *J. Organomet. Chem.* 289 (1985) 117–131.

[8] (a) K. M. E. Burton, D. A. Pantazis, R. G. Belli, R. McDonald, L. Rosenberg, *Organometallics* 35 (2016) 3970–3980; (b) V. Cadierno, J. Díez, M. Pilar Gamasa, J. Gimeno, E. Lastra, *Coord. Chem. Rev.* 193–195 (1999) 147–205; (c) M. Pilar Gamasa, J. Gimeno, C.

Gonzalez-Bernardo, B. M. Martín-Vaca, D. Monti, M. Bassetti, *Organometallics* 15 (1996) 302–308.

[9] Examples: (a) I. García de la Arada, J. Díez, M. Pilar Gamasa, E. Lastra *Organometallics* 34 (2015) 1345–1353; (b) I. García de la Arada, J. Díez, M.P. Gamasa, E. Lastra *J. Organomet. Chem.* 797 (2015) 101–109.

[10] (a) S. Nolan, *Acc. Chem. Res.* 47 (2014) 3089–3101; (b) C. A. Mebi, R. P. Nair, B. J. Frost, *Organometallics* 26 (2007) 429–438; (c) K. Bieger, J. Díez, M. Pilar Gamasa, J. Gimeno, M. Pavlišta, Y. Rodríguez-Álvarez, S. García-Granda, R. Santiago-García, *Eur. J. Inorg. Chem.* (2002) 1647–1656; (d) P. Alvarez, J. Gimeno, E. Lastra, S. García-Granda, J. F. Van der Maelen, M. Bassetti, *Organometallics* 20 (2001) 3762–3771; (e) E. P. Kündig, C. M. Saudan, V. Alezra, F. Viton, G. Bernardinelli, *Angew. Chem. Int. Ed.* 40 (2001) 4481–4485; (f) M. Bassetti, S. Marini, F. Tortorella, V. Cadierno, J. Díez, M. Pilar Gamasa, J. Gimeno, *J. Organomet. Chem.* 593–594 (2000) 292–298; (g) Y. Yamamoto, H. Kitahara, R. Hattori, K. Itoh, *Organometallics* 17 (1998) 1910–1912.

[11] (a) M. José Calhorda, L. F. Veiros, *Dalton Trans.* 40 (2011) 11138–11146; (b) M. José Calhorda, C. C. Romão, L. F. Veiros, *Chem. Eur. J.* 8 (2002) 868–875; (c) L. F. Veiros, *Organometallics* 19 (2000) 3127–3136; (d) J. M. O’Connor, C. P. Casey, *Chem. Rev.* 87 (1987) 307–318; (e) J. W. Faller, R. H. Crabtree, A. Habib, *Organometallics* 4 (1985) 929–935.

[12] (a) M. J. Stark, M. J. Shaw, N. P. Rath, E. B. Bauer, *Eur. J. Inorg. Chem.* (2016) 1093–1102; (b) M. J. Queensen, J. M. Rabus, E. B. Bauer, *J. Mol. Cat. A: Chem.* 407 (2015) 221–229; (c) M. J. Queensen, N. P. Rath, E. B. Bauer, *Organometallics* 33 (2014) 5052–5065; (d) D. F. Alkhaleeli, K. J. Baum, J. M. Rabus, E. B. Bauer, *Catal. Commun.* 47 (2014) 45–48; (e)

A. K. Widaman, N. P. Rath, E. B. Bauer, *New J. Chem.* 35 (2011) 2427–2434; (f) S. Costin, A. K. Widaman, N. P. Rath, E. B. Bauer, *Eur. J. Inorg. Chem.* (2011) 1269–1282; (g) S. Costin, N. P. Rath, E. B. Bauer, *Tetrahedron Lett.* 50 (2009) 5485–5488; (h) S. Costin, S. L. Sedinkin, E. B. Bauer, *Tetrahedron Lett.* 50 (2009) 922–925; (i) S. Costin, N. P. Rath, E. B. Bauer, *Adv. Synth. Catal.* 350 (2008) 2414–2424.

[13] Representative examples: (a) O. bin Shawkataly, M. A. A. Pankhi, M. G. Alam, C. S. Yeap, H.-K. Fun, *Polyhedron* 30 (2011) 444–450; (b) R. Corrêa da Costa, F. Hampel, J. A. Gladysz, *Polyhedron* 26 (2007) 581–588.

[14] (a) A. C. Marr, M. Nieuwenhuyzen, C. L. Pollock, G. C. Saunders, *Organometallics* 26 (2007) 2659–2671; (b) F. Zhao, Y. Ikushima, M. Chatterjee, O. Sato, M. Arai, *J. Supercrit. Fluids* 27 (2003) 65–72.

[15] A. K. Renfrew, R. Scopelliti, P. J. Dyson, *Inorg. Chem.* 49 (2010) 2239–2246.

[16] D. Gudmunsen, E. G. Hope, D. R. Paige, A. M. Stuart *J. Fluorine Chemistry* 130 (2009) 942–950.

[17] R. Tuba, R. Corrêa da Costa, H. S. Bazzi, J. A. Gladysz, *ACS Catal.* 2 (2012) 155–162.

[18] S. Costin, N. P. Rath, E. B. Bauer *Inorg. Chem. Commun.* 14 (2011) 478–480.

[19] E. J. Derrah, J. C. Marlinga, D. Mitra, D. M. Friesen, S. A. Hall, R. McDonald, L. Rosenberg, *Organometallics* 24 (2005) 5817–5827.

[20] M. Kamigaito, Y. Watanabe, T. Ando, M. Sawamoto, *J. Am. Chem. Soc.* 124 (2002) 9994–9995.

[21] (a) C. R. Martinez, B. L. Iverson, *Chem. Sci.* 3 (2012) 2191–2201; (b) C. Janiak J. Chem. Soc., Dalton Trans. (2000) 3885–3896.

[22] (a) J. Lodinský, J. Vinklársek, L. Dostál, Z. Růžičková, J. Honzíček, *RSC Adv.* 5 (2015) 27140–27153; (b) J. Honzíček, J. Vinklársek, M. Erben, J. Lodinský, L. Dostál, Z. Padělkova, *Organometallics* 32 (2013) 3502–3511.

[23] S. Costin, N. P. Rath, E. B. Bauer, *Inorg. Chim. Acta* 362 (2009) 1935–1942.

[24] (a) B. Suthar, A. Aldongarov, I. S. Irgibaeva, M. Moazzen, B. T. Donovan-Merkert, J. W. Merkert, T. A. Schmedake, *Polyhedron* 31 (2012) 754–758; (b) A. P. Shaw, J. R. Norton, D. Buccella, L. A. Sites, S. S. Kleinbach, D. A. Jarem, K. M. Bocage, C. Nataro, *Organometallics* 28 (2009) 3804–3814; (c) A. R. O'Connor, C. Nataro, A. L. Rheingold, J. *Organomet. Chem.* 679 (2003) 72–78; (d) S. Santi, L. Broccardo, M. Bassetti, P. Alvarez, *Organometallics* 22 (2003) 3478–3484.

[25] General examples and reviews regarding the nucleophilic substitution of propargylic alcohols: (a) K. Nakajima, M. Shibata, Y. Nishibayashi *J. Am. Chem. Soc.* 137 (2015) 2472–2475; (b) D.-Y. Zhang, X.-P. Hu, *Tetrahedron Lett.* 56 (2015) 283–295; (c) B. Wang, C. Liu, H. Guo, *RSC Adv.* 4 (2014) 53216–53219; (d) F.-Z. Han, F.-L. Zhu, Y.-H. Wang, Y. Zou, X.-H. Hu, S. Chen, X.-P. Hu, *Org. Lett.* 16 (2014) 588–591; (e) Eike B. Bauer, *Synthesis* 44 (2012) 1131–1151; (f) Y. Nishibayashi, *Synthesis* 44 (2012) 489–503; (g) R. J. Detz, H. Hiemstra, J. H. van Maarseveen, *Eur. J. Org. Chem.* (2009) 6263–6276; (h) N. Ljungdahl, N. Kann, *Angew. Chem. Int. Ed.* 48 (2009) 642–644.

[26] (a) B. Schmidt, *Eur. J. Org. Chem.* (2004) 1865–1880; (b) M. B. Dinger, J. C. Mol, *Organometallics* 22 (2003) 1089–1095.

[27] (a) A. B. P. Lever, *Coord. Chem. Rev.* 254 (2010) 1397–1405; (b) C. Slugovc, E. Růba, R. Schmid, K. Kirchner, K. Mereiter, *Monatsh. Chem.* 131 (2000) 1241–1251.

[28] S. S. Keisham, Y. A. Mozharivskyj, P. J. Carroll, M. R. Kollipara, *J. Organomet. Chem.* 689 (2004) 1249–1256.

[29] Representative examples: (a) S. L. Kuan, W. K. Leong, R. D. Webster, L. Y. Goh, *Organometallics* 31 (2012) 5159–5168; (b) A. Yoshinari, A. Tazawa, S. Kuwata, T. Ikariya, *Chem. Asian J.* 7 (2012) 1417–1425; (c) W. M. Khairul, M. A. Fox, N. N. Zaitseva, M. Gaudio, D. S. Yufit, B. W. Skelton, A. H. White, J. A. K. Howard, M. I. Bruce, P. J. Low, *Dalton Trans.* (2009) 610–620; (d) S. Nagao, H. Seino, M. Hidai, Y. Mizobe, *Dalton Trans.* (2005) 3166–3172; (e) J. Matthes, S. Gründemann, A. Toner, Y. Guari, B. Donnadieu, J. Spandl, S. Sabo-Etienne, E. Clot, H.-H. Limbach, B. Chaudret, *Organometallics* 23 (2004) 1424–1433.

[30] J. S. Valentine, *Chem. Rev.* 73 (1973) 235–245.

[31] (a) T. T. da Cunha, F. Pointillart, B. Le Guennic, C. L. M. Pereira, S. Golhen, O. Cador, L. Ouahab, *Inorg. Chem.* 52 (2013) 9711–9713; (b) L. Terborg, S. Nowak, S. Passerini, M. Winter, U. Karst, P. R. Haddad, P. N. Nesterenko, *Anal. Chim. Acta* 714 (2012) 121–126; (c) N. R. Brooks, A. J. Blake, N. R. Champness, J. W. Cunningham, P. Hubberstey, M. Schröder, *Cryst. Growth Des.* 1 (2001) 395–399; (d) M. Di Vaira, M. Peruzzini, S. S. Costantini, P. Stoppioni, *J. Organomet. Chem.* 691 (2006) 3931–3937.

[32] F. Barrière, W. E. Geiger, *J. Am. Chem. Soc.* 128 (2006) 3980–3989.

[33] Bruker Analytical X-Ray, Madison, WI, 2016

[34] G. M. Sheldrick, *Acta Cryst. A* 64 (2008) 112–122.

[35] S. Parsons, H. Flack, *Acta Cryst.* A60 (2004) s61.

[36] A. L. Spek, *Acta Cryst.* A46 (1990) C34.